Crystallization kinetics of poly(*p*-phenylene sulphide): effect of molecular weight

Leonardo C. López and Garth L. Wilkes
Department of Chemical Engineering, Polymer Materials and Interfaces Laboratory, Virginia Polytechnic Institute and State University, Blacksburg, Virginia 24061, USA
(Received 27 February 1987; accepted 13 June 1987)

The crystallization behaviour of poly(*p*-phenylene sulphide) (PPS) has been studied in terms of linear crystal growth rates and overall rates of bulk crystallization as functions of molecular weight and temperature. In addition, nucleation densities were estimated for PPS crystallized from the melt. The overall rate of bulk crystallization was described by the Avrami equation. In the range of molecular weights studied (24 000–63 000), crystal growth rates and overall rates of bulk crystallization decreased as the molecular weight increased. However, the effect was not particularly large. The estimated nucleation densities indicated a decrease by a factor of 32 as the molecular weight decreased. The linear crystal growth rate data were analysed in terms of several proposed models. The data seemed to conform very well to an 'inverse' logarithmic function of the number-average molecular weight recently proposed by Cheng and Wunderlich.

(Keywords: poly(phenylene sulphide); crystallization; molecular weight; crystallization kinetics)

INTRODUCTION

Poly(*p*-phenylene sulphide) (PPS) is an important high strength/high temperature engineering thermoplastic that is finding increasing use in technological applications such as moulding resins, fibres and matrices for thermoplastic composites. It has a glass transition temperature of about 85°C and a melting point at about 285°C. An unusual combination of properties[1,2] allows the use of PPS in pump impellers, ball valves, wear rings, electrical sockets, battery and telephone components, chip carriers, optical-fibre cables and electronic component encapsulants[3,4]. Recently, it has been rendered electrically conductive by addition of dopants[5–7].

The properties of semicrystalline polymers such as PPS depend on the crystallization behaviour of the polymer. Therefore, the study of the morphology and kinetics of crystallization is of major importance. A few studies have focused on these two points[8–12]. In a previous publication, the authors reported on the morphological textures of PPS as observed by utilizing an etching technique to enhance the details of the spherulitic structure[13]. The technique was based on the more rapid chemical degradation of amorphous PPS by an anhydrous aluminium chloride suspension in toluene. The technique required very careful control of the concentration of aluminium chloride, temperature and atmospheric medium. Spherulitic superstructures with fine radial fibrils were observed in thin films crystallized from the molten state. Spherulites that had nucleated close to the film surface and showed disc-like appearance presented 'fibrils' growing from the spherulite centre in a spiral form in the first few microns, with further growth continued in a radial fashion. In addition, spherulites that had impinged indicated a very good interfacing of the crystalline fibrils of one spherulite with those of the neighbouring one. Continuing the studies on the crystallization behaviour of PPS, the present work reports on the crystallization kinetics of PPS studied by differential scanning calorimetry and polarized light microscopy. In particular, the effect of molecular weight on the crystallization rates is reported here, while the effects of addition of the branching agent, trichlorobenzene, during polymerization, and the chemical nature of the chain terminal moieties will be given in a forthcoming paper.

EXPERIMENTAL

Three samples of PPS kindly donated and characterized by Dr C. J. Stacy of Phillips Petroleum Co. were utilized in this study. The sample designation and characteristics are shown in *Table 1*.

Growth rate measurements

PPS specimens were moulded into thin films between glass cover slips to measure spherulitic growth rates. A Zeiss polarizing microscope equipped with a Leitz 350 heating stage and a 35 mm camera was utilized. Temperature calibration of the heating stage was performed with naphthalene, indium, anthraquinone and sodium nitrate.

PPS is known to undergo chemical reactions at high temperature in the presence of oxygen that involve chain extension, branching and crosslinking[14]. These reactions

Table 1 Characteristics of samples utilized to study the effect of molecular weight on the crystallization kinetics of PPS

Sample designation	$\langle M_w \rangle$	$\langle M_w \rangle / \langle M_n \rangle$
PPS24	24 000	1.4
PPS49	49 000	1.4
PPS63	63 000	1.5

0032-3861/88/010106-08$03.00

alter the molecular weight of PPS. Therefore, the residence times of samples at high temperature need to be minimized. Moreover, the crystallization studies must be conducted under a nitrogen atmosphere to minimize the extent of these reactions. For this reason, the samples were held at 320°C for 4 min prior to crystallization. Crystallizations were performed in the temperature range 220 to 260°C, minimizing the residence times of the samples at high temperatures as much as possible. No crystallization time was longer than 90 min. This limitation on the temperature range impaired a further detailed analysis of the growth rates in terms of the regime theory proposed by Hoffman and coworkers[15-17]

Spherulite growth was followed by taking photographs with a 35 mm camera at fixed time intervals. The spherulite diameters were measured from these optical micrographs. The crystal growth rates were determined by plotting spherulitic radius as a function of time and determining the slope of the straight lines. Reproducibility of the growth rate measurements indicated a deviation $<10\%$.

Rate of bulk crystallization

A Perkin-Elmer DSC-4 differential scanning calorimeter was utilized to obtain bulk crystallization isotherms. The temperature calibration was performed with an indium standard and anthraquinone. The PPS samples were weighed in aluminium pans (2–3 mg) and were crystallized from the melt after being held at 320°C for 4 min.

Crystallization from the melt was only possible in the temperature range 220–260°C. Two factors contributed to limit this temperature range. The upper end was set by the long residence time needed to complete crystallization at high temperatures, which may induce chemical reactions. The lower limit was imposed by the high nucleation densities encountered. For this reason, the cooling rates available in the DSC-4 were not sufficiently fast to permit the achievement of temperatures lower than 220°C prior to the initiation of crystallization.

In order to obtain crystallization data in the diffusion controlled part of the crystallization rate–temperature curve, thin amorphous PPS films were formed. These were prepared by compression moulding PPS at 320°C for 4 min at 2000 lb/in^2, and quenching in ice water. Similar to crystallization from the melt, the temperature range for crystallization from the glassy state was very limited.

Data analysis

The overall rate of bulk crystallization was analysed in terms of the well known Avrami equation[18]:

$$X_c(t)=1-e^{-Kt^n} \tag{1}$$

In this equation, $X_c(t)$ is the volume fraction of crystals at time t; K is a rate constant that includes the temperature dependent terms, and contains information regarding diffusion and nucleation rates; n, the Avrami exponent is a constant dependent on the types of processes occurring during nucleation and growth. Assuming that nucleation results in three-dimensional spherulites, and that the increase in crystal dimensions is linear with crystallization time, the nucleation density N (number of nuclei/cm^3) can be estimated by:

$$N=\frac{3K}{4\pi G^3} \tag{2}$$

where K is obtained from equation (1) and G is the linear crystal growth rate. Therefore, the combination of K obtained from d.s.c. experiments and G obtained from polarized light microscopy experiments on spherulitic growth rates allows the estimation of the nucleation density as a function of crystallization temperature.

The parameters in equation (1) can be determined by twice taking the logarithm of this equation,

$$\ln[-\ln(1-X_c(t)]=\ln K+n\ln t \tag{3}$$

Consequently, a plot of the double logarithm of the amorphous content as a function of the logarithm of time (a classical Avrami plot) permits the determination of K from the intercept, and n from the slope of the straight line. However, due to the lack of sensitivity of a double logarithmic plot, the method would be suspected of being not highly accurate.

A potentially more precise method to determine n and K involves the use of the crystallization half-time. Referring to *Figure 1*, the whole area under the exothermic curve represents a normalized crystalline content of unity. On a normalized basis, the crystallization half-time, $t_{1/2}$, is defined as the time at which the normalized crystalline content is 0.5. The crystallization half-time method consists of the determination of the crystallization half-time, $t_{1/2}$, from a graph of the amorphous content as a function of time, and the calculation of the slope, S, of the curve of amorphous content as a function of logarithm of time at $t=t_{1/2}$.

Taking the logarithm of equation (1) at $t=t_{1/2}$, one obtains[19],

$$K=\frac{\ln 2}{t_{1/2}^n} \tag{4}$$

The slope of the curve $(1-X_c(t))$ as function of $\ln(t)$ can be written as follows:

$$S=t\frac{\partial(1-X_c(t))}{\partial t} \tag{5}$$

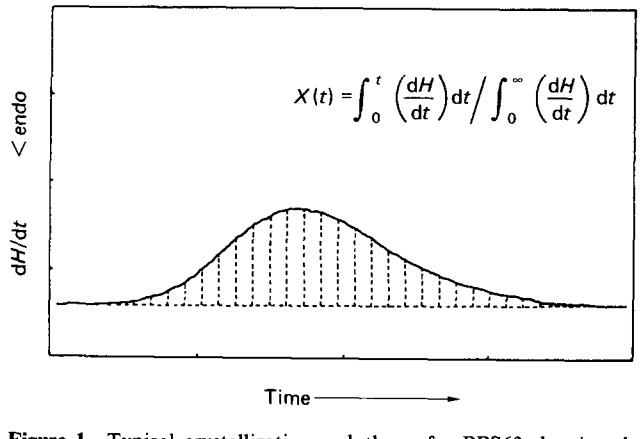

Figure 1 Typical crystallization endotherm for PPS63 showing the method utilized to calculate the normalized crystalline content

Table 2 Avrami exponent determined by the double logarithmic, and by the crystallization half-time methods for PPS49

	Avrami exponent	
Temperature (°C)	$\ln[-\ln(1-X)]$ vs. $\ln t$	$t_{1/2}$ method
255	2.9	3.0
250	3.0	3.1
245	2.8	2.6
240	2.7	2.9
235	2.7	2.8
230	2.7	2.8
225	2.8	2.9
220	2.8	2.8

Using equation (1), $\partial(1-X_c(t))/\partial t$ can be calculated:

$$\frac{\partial(1-X_c(t))}{\partial t} = -Knt^{n-1}\,e^{-Kt^n} \tag{6}$$

At $t=t_{1/2}$ it can be shown that:

$$S_{t_{1/2}} = \frac{n\ln 2}{2} \tag{7}$$

Therefore, using equations (4) and (7) the two parameters of the Avrami equation, K and n can be determined.

Both methods discussed so far were used to determine the parameters of the Avrami equation. As shown in *Table 2*, the Avrami exponents calculated with both methods compare very favourably. This indicates that, surprisingly, the methods are equally precise, and adds a greater degree of confidence in the values obtained. In addition, reproducibility of the determination of the rate constant, K, indicated a per cent deviation of 10%.

In particular, when differential scanning calorimetry is used to follow bulk crystallization, the weight fraction of material that has crystallized at time t, $X_c(t)$, is given by:

$$X_c(t) = \frac{\int_0^t \left(\frac{dH}{dt}\right) dt}{\int_0^\infty \left(\frac{dH}{dt}\right) dt} \tag{8}$$

where dH/dt is the rate of heat evolution as a function of time. This is achieved by determining the area under the crystallization isotherm point by point, and taking the ratio of the areas at each time interval to the total area. This method is depicted schematically in *Figure 1*.

RESULTS AND DISCUSSION

Crystal growth rates are presented in *Figure 2* in the form of plots of the logarithm of growth rate as function of crystallization temperature. Slower crystal growth rates are observed as the molecular weight of PPS increases. This is reasonable since increasingly longer chains need more cooperative displacements to go from the melt to the crystalline structure. Therefore, the time necessary to crystallize increases, and the crystal growth rate decreases. At a supercooling of 70°C, the lowest molecular weight PPS24 ($\langle M_w\rangle = 24\,000$) has a crystal growth rate four times faster than the highest molecular weight PPS63 ($\langle M_w\rangle = 63\,000$). However, the difference between PPS49 ($\langle M_w\rangle = 49\,000$) and PPS63 is only a factor of 0.5. This may indicate that the decrease in growth rate due to increased molecular weight may be approaching a limiting value.

Figure 3 shows a plot of the normalized crystalline content of PPS49 crystallized from the melt as a function of the logarithm of time, and an Avrami plot, i.e. a graph of $\ln[-\ln(1-X_c(t))]$ versus logarithm of time. These graphs were calculated using equations (8) and (3), respectively. As can be seen in *Figure 3b*, the d.s.c. data follow almost perfectly the Avrami equation for the overall rate of bulk crystallization. The values of the Avrami exponents corresponding to samples crystallized from the melt are shown in *Figure 4* as a function of the crystallization temperature. It is clear that PPS49 and PPS63 present Avrami exponents very close to 3. This strongly indicates that the assumption behind equation (2), namely that three-dimensional spherulites are formed, is valid for the calculation of the nucleation densities. PPS24, however, shows lower values of n of the order of 2.5. These lower values may be attributed to growth that is not three-dimensional, which lowers the value of the Avrami exponent. Consider *Figure 5*, which presents a schematic representation of the development of a spherulite from a single lamella (step 1) to a three-dimensional spherulite (step 5). The intermediate sheaf-like structures such as those in steps 3 and 4 in *Figure 5* would decrease the Avrami exponent from the value of 3. Consequently, the presence of these structures would contribute to the lowering of n in PPS24. However, observations in the optical microscope indicated the formation of spherulitic textures in PPS24. Another possible cause of a somewhat lower Avrami exponent exists. Specifically, it has been shown that n may be lowered as much as 0.3 due to the impossibility of achieving a constant volume transformation, an assumption imposed in the derivation of equation (1)[20].

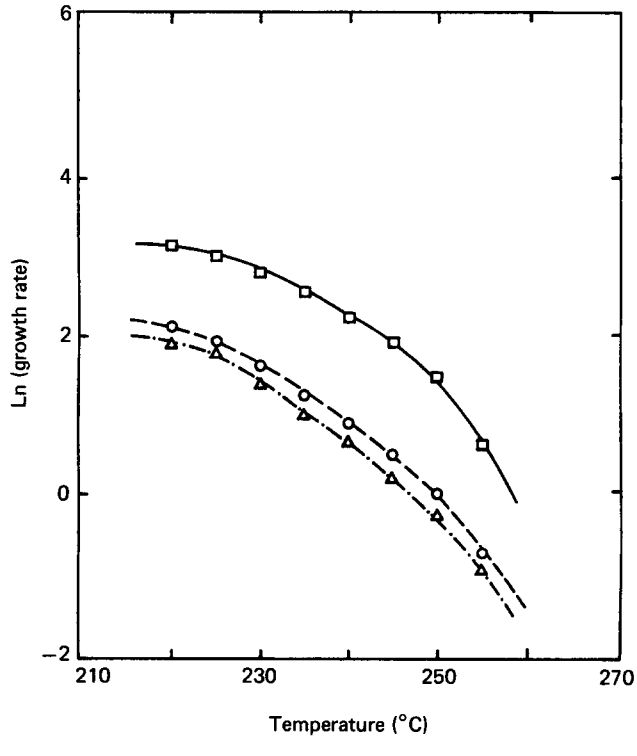

Figure 2 Relationship between linear crystal growth rate ($\mu m\ min^{-1}$) and crystallization temperature (°C) for PPS samples crystallized from the melt. $\bar{M}_\omega$: □, 24 000; ○, 49 000; △, 63 000

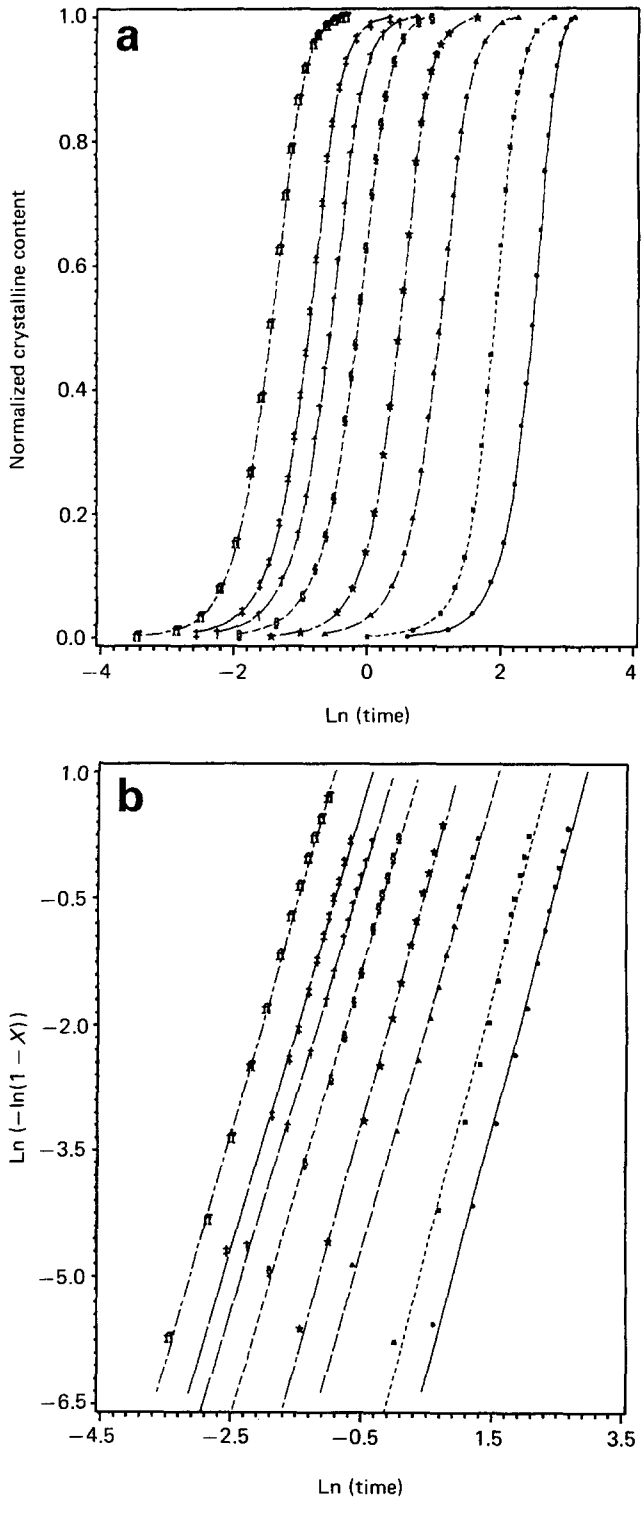

Figure 3 Crystallization isotherms (time in min) corresponding to PPS49. (a) Normalized crystalline content as a function of ln(time). (b) Double logarithmic plot of amorphous content versus ln(time), following the Avrami equation. T_c (°C): ●, 255; ■, 250; △, 245; ★. 240; §, 235, †, 230; ‡, 225, ff, 220

In *Figure 6*, the logarithm of K and the logarithm of $t_{1/2}$ are represented as functions of the crystallization temperature. The complete curves are presented. However, as expressed in the Experimental section, there were limitations in the temperature ranges studied. No reliable data points could be gathered in the region of fast crystallization rates due to the start of crystallization at rapid rates before temperature stabilization could be achieved. Therefore, the curves were constructed following a third-order polynomial regression. Although from a statistical point of view these curves should be considered cautiously in their central part, the rate maxima located at 170°C for PPS24 and PPS49, and at 180°C for PPS63 are in good agreement with the values obtained by Jog and Nadkarni[8], and by Lovinger, Davis and Padden[9]. *Figure 6* shows that ln K and ln $t_{1/2}$ curves also present the effect of molecular weight. At a supercooling of 70°C, the overall rate of bulk crystallization decreases by a factor of 3.5 as the molecular weight of PPS increases from 24 000 to 63 000. Similarly, the crystallization half-time increases by a factor of 3.5 as the molecular weight increases. It is of interest to compare these factors to those corresponding to poly(ethylene terephthalate) (PET) in view of their similar window for crystallization. PET has a glass transition temperature (T_g) at about 69°C and a melting temperature (T_m) at about 265°C. Therefore, the temperature range in which PET can crystallize is similar to that of PPS ($T_g = 85$°C, $T_m = 285$°C). In addition, PPS can potentially substitute PET in many applications, especially if chemical resistance is of importance. Van Antwerpen and van Krevelen[21] studied the effect of molecular weight on the crystallization kinetics of PET in a similar range of $\langle M_n \rangle$ as that of PPS reported here. They observed that at a supercooling of 90°C, the overall rate of crystallization as measured by the crystallization half-time decreased by only a factor of 2.5 as the $\langle M_n \rangle$ of PET increased from 19 000 to 35 400. Therefore, the effect of molecular weight on the overall rate of bulk crystallization seems to be more important in PPS than in PET.

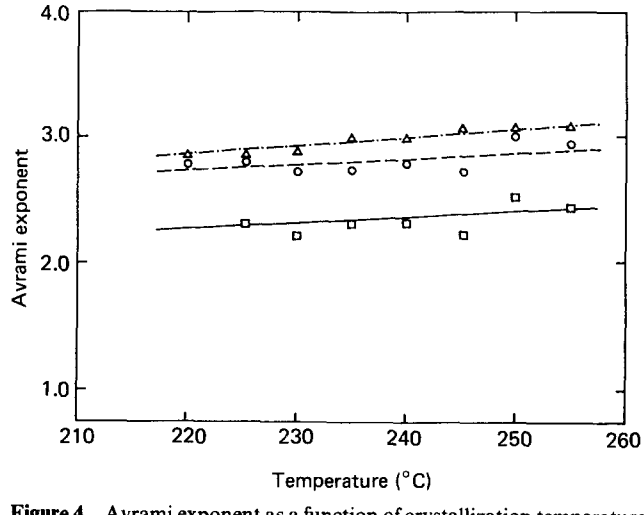

Figure 4 Avrami exponent as a function of crystallization temperature for PPS crystallized from the melt. $\bar{M}_\omega$: □, 24 000; ○, 49 000; △, 63 000

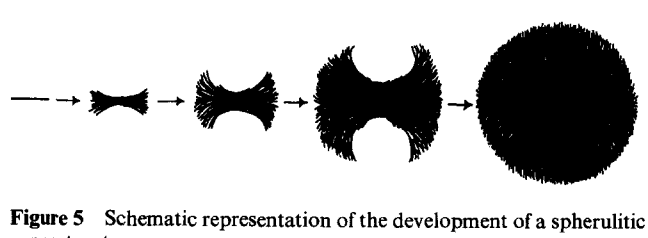

Figure 5 Schematic representation of the development of a spherulitic superstructure

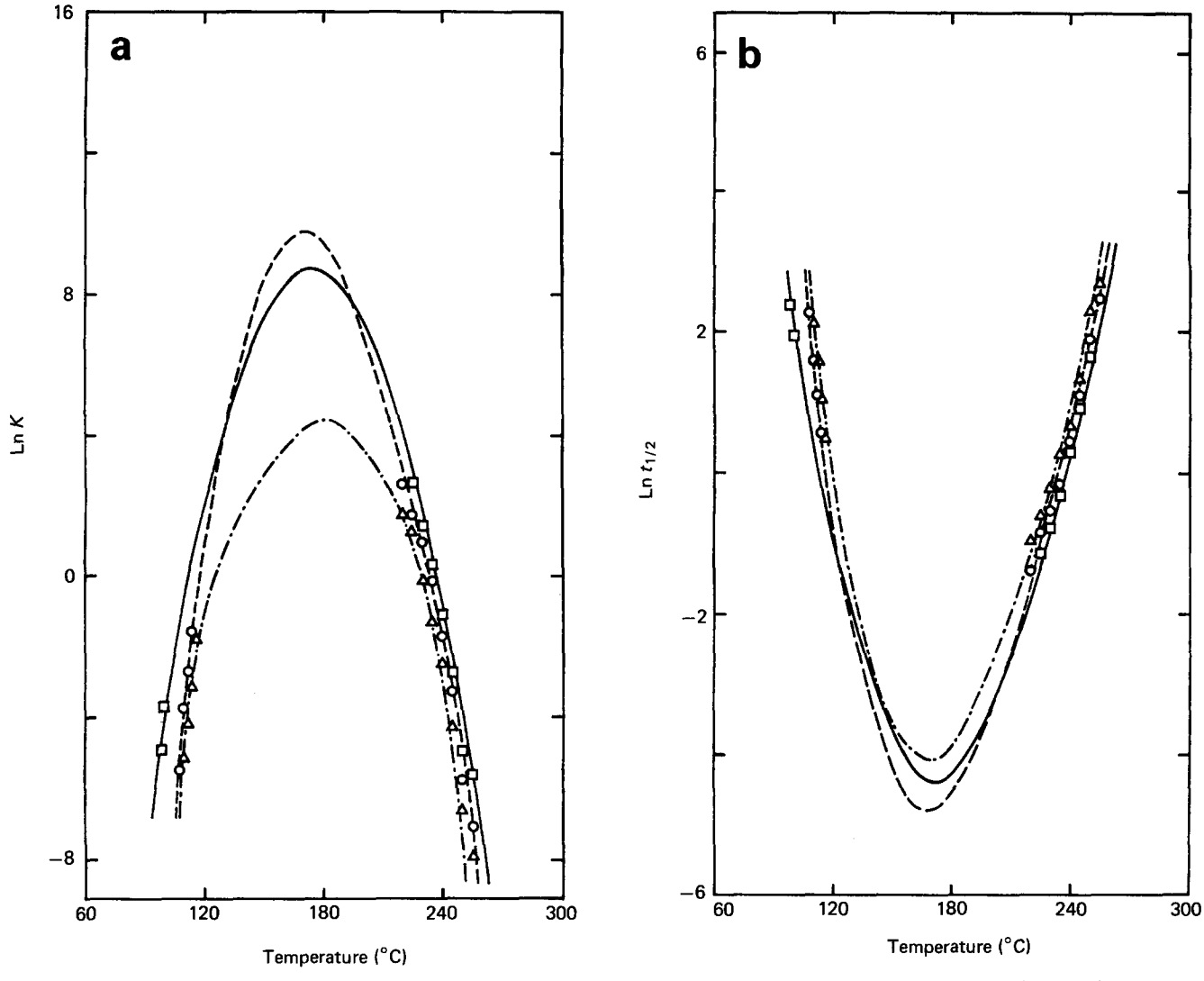

Figure 6 (a) Relationship between rate constant, K, and crystallization temperature; (b) relationship between crystallization half-time (min) and crystallization temperature, for different molecular weight materials, $\bar{M}_\omega$: □, 24 000; ○, 49 000; △, 63 000

Combination of the growth rate data and overall rate of bulk crystallization data permits the calculation of the nucleation density by means of equation (2). The results of these calculations are plotted in *Figure 7* as a function of the crystallization temperature for samples crystallized from the melt. These show that the nucleation density decreases as the crystallization temperature increases in all cases, as expected. However, the lower molecular weight PPS24 has nucleation density values that are 32-fold lower than the higher molecular weight PPS49 and PPS63. This indicates that the faster overall rate of bulk crystallization of PPS24 is due primarily to rapid crystal growth rates and is not due to higher nucleation densities.

Figure 8 presents a plot of the normalized overall heat of crystallization as a function of T_c for PPS crystallized from the melt. The heat of crystallization follows the usual increasing trend with crystallization temperature. There is about a 30% increase in the heat of crystallization as the temperature varies from 220 to 255°C for all samples studied. The higher molecular weight PPS, PPS49 and PPS63 have similar values for the heat of crystallization. However, PPS24 shows somewhat higher values of ΔH at low crystallization temperatures, indicating a higher crystalline content. At temperatures above 250°C the heats of crystallization have similar values.

Crystal growth rate as a function of molecular weight

In classical crystallization theory, the crystal growth rate is expressed as:[22]

$$\ln G = \ln G_0 - \frac{\Delta E}{kT} - \frac{\Delta F^*}{kT} \qquad (9)$$

where ΔE represents the free energy of activation for the transport of units across the phase boundary; ΔF^* is the free energy of activation for the formation of a critical size nucleus; k is the Boltzmann constant; and T represents the absolute temperature. Several attempts have been made to introduce a molecular weight dependence into equation (9). For example, Devoy and Mandelkern[23] analysed the molecular weight dependence of G considering the effect of chain length on the free energy of fusion. That is, only the last term in equation (9), ΔF^*, was considered a function of molecular weight. It was also suggested that the growth rate is inversely proportional to $\langle M_n \rangle$. Therefore, Lovering[24] added a $-\ln\langle M_n \rangle$ term to the right-hand side of equation (9) to explain the molecular weight dependence of G. This same author showed that a plot of $\ln G + \ln\langle M_n \rangle$ as a function of $T_m/T_c(T_m^0 - T_c)$ should provide a straight line with all his data for different molecular weights falling on the

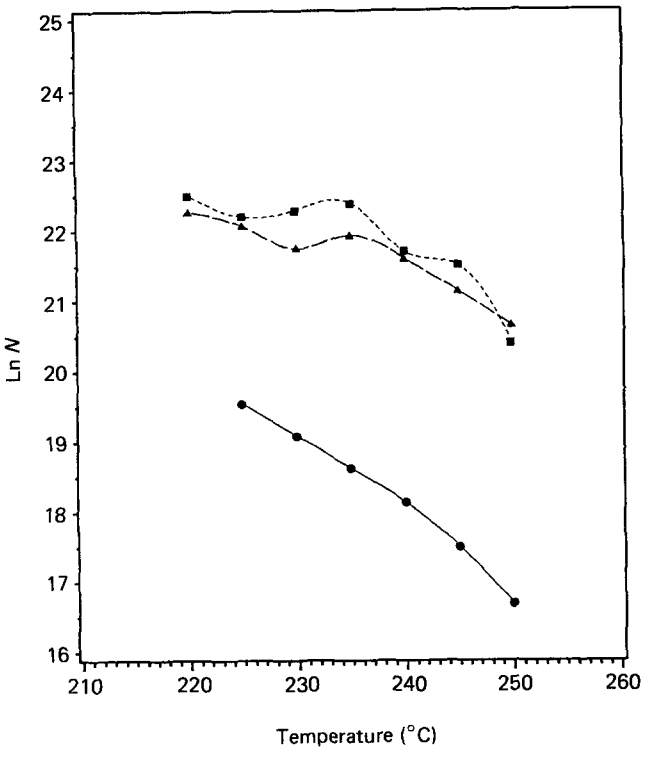

Figure 7 Plot of nucleation density (N is number of nuclei/cm^3) as a function of crystallization temperature for different molecular weights of PPS crystallized from the melt. $\bar{M}_\omega$: ●, 24000; ■, 49000; ▲, 63000

same line. In contrast, Hoffman and Weeks[25] suggested that the term G_0 was the molecular weight dependent parameter. They proposed that G_0 was proportional to $(1/\langle n\rangle)^y$, where $\langle n\rangle$ is the number-average degree of polymerization, and y takes values between zero and unity. Recently, Hoffman[26] stated that the linear crystal growth rate (G) was found to be inversely proportional to $\langle n_z\rangle$, the z-average degree of polymerization.

Some empirical functions have also been suggested as attempts to express the molecular weight dependence of G. As an example, Magill and Li[27] proposed an equation of the form,

$$\ln G = \frac{a}{\langle M_n\rangle^\alpha} \tag{10}$$

where a is a constant, $\langle M_n\rangle$ is the number average molecular weight and α has values $0.5 < \alpha < 1.2$.

Recently, Cheng and Wunderlich[28] presented a logarithmic function to fit the molecular weight dependence of the crystal growth rate of poly(ethylene oxide) in the very wide range of $\langle M_w\rangle$ 3500–5 000 000:

$$\ln G = b \ln\langle M_n\rangle + a \tag{11}$$

This model also seemed to fit other literature data corresponding to polyethylene, poly(hexamethylene oxide), poly(ethylene terephthalate), poly(tetramethyl-*p*-silphenylene)siloxane and *trans*-1,4-poly(2-methyl butadiene). The connotations behind this model, as stated by Cheng and Wunderlich, indicate that molecular nucleation controls the crystal growth rather than crystal secondary nucleation. Moreover, since the $\exp[1/(T_m^0 - T_c)]$ and $\exp[1/T_c(T_m^0 - T_c)]$ dependences describe surface nucleation, these same authors suggested that a molecular nucleus involves: 'a surface patch of increased surface area and a cooperative molecular weight dependent term.'

Although the range of molecular weights studied in the present report is narrow, the molecular weight dependence of G was analysed. The data were analysed in terms of the models by Lovering[24], Hoffman[26], Magill and Li[27], and Cheng and Wunderlich[28]. Only the latter model seems to conform to the data well as will be demonstrated.

Since the thermodynamic melting points, T_m^0, were needed for this analysis, they were determined by the method of Hoffman and Weeks[29]. *Figure 9* shows typical Hoffman–Weeks plots, i.e. plots of melting point as function of crystallization temperature. The values obtained for the thermodynamic melting points are 304°C for PPS24, 308°C for PPS49, and 312°C for PPS63.

As expressed before, Lovering's model[24] implies that a plot of $\ln G + \ln\langle M_n\rangle$ as a function of $T_m/T_c(T_m^0 - T_c)$ should give a straight line with all the data for different $\langle M_n\rangle$ on the same line. The present data, when plotted in this way, fell into straight lines; however, the lines were far from being coincident. When the data were analysed in terms of Hoffman's model[26] ($G \propto 1/\langle n_z\rangle$), the data did not conform to this relationship. Gel permeation chromatography data[30] which provided $\langle n_z\rangle$ showed that the exponents on $\langle n_z\rangle$ were higher than 1.7 in all cases, and the correlation coefficients were very low, i.e. the linear relationship was very poor. Similarly, in the case of the model by Magill and Li[27], the values of the exponent α were very high, and the relationship was very poor, as was observed in low values of the correlation coefficients.

Figure 10 presents a graph of linear crystal growth rates as function of supercooling $\Delta T = T_m^0 - T_c$. By taking

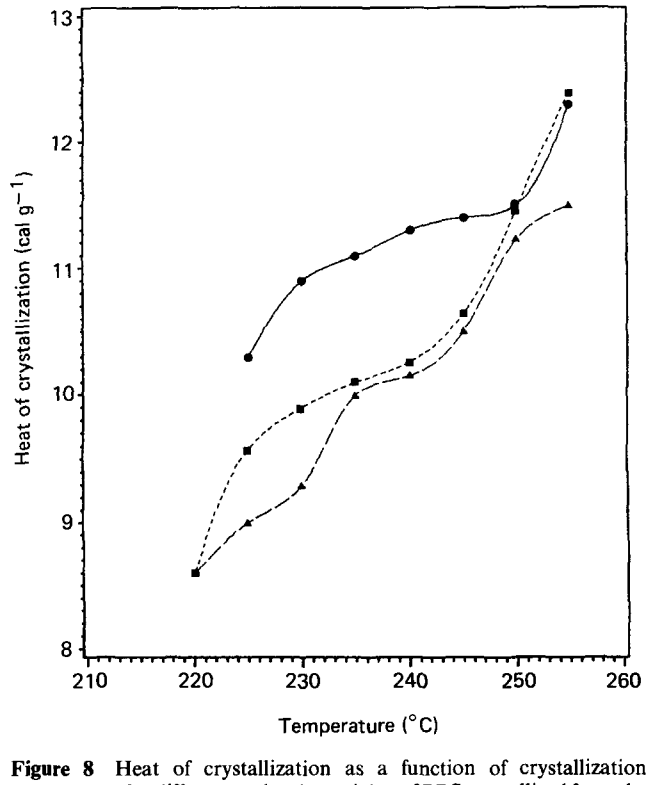

Figure 8 Heat of crystallization as a function of crystallization temperature for different molecular weights of PPS crystallized from the melt. $\bar{M}_\omega$: ●, 24000; ■, 49000; ▲, 63000

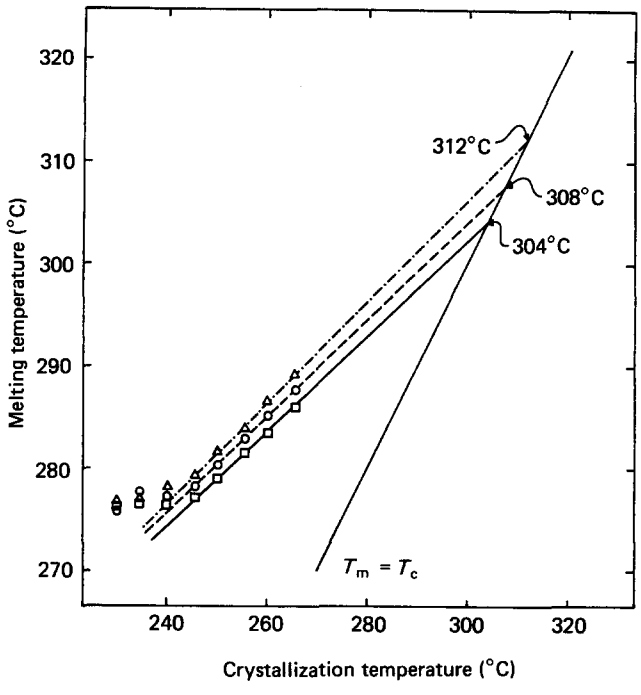

Figure 9 Hoffman–Weeks plots utilized to determine thermodynamic melting points of different molecular weight fractions of PPS. $\bar{M}_\omega$: □, 24000; ○, 49000; △, 63000

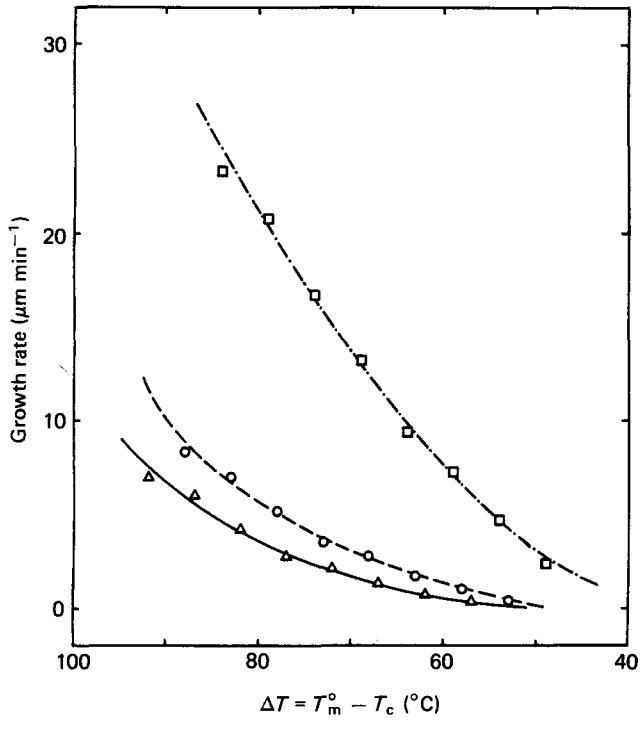

Figure 10 Linear crystal growth rates of PPS as functions of the supercooling $\Delta T = T_m^0 - T_c$. $\bar{M}_\omega$: □, 24000; ○, 49000; △, 63000

values of G at constant supercooling for the different molecular weights from *Figure 10*, equation (11) can be represented. *Figure 11* shows a plot of logarithm of G as a function of logarithm of $\langle M_n \rangle$ for a series of supercoolings. The data fall very well on straight lines that conform with equation (11). Furthermore, *Figure 12* indicates that the slope increases and the intercept decreases as the supercooling increases in a similar way to the data of Cheng and Wunderlich on poly(ethylene oxide)[28]. In addition, the slope and the intercept are linear functions of $1/\Delta T$ and $1/T_c \Delta T$, respectively. Therefore, it seems that the data presented in this report give another example that follows the model proposed by Cheng and Wunderlich[28] and gives further support to their hypothesis regarding the dependence of the linear crystal growth rate on molecular weight.

CONCLUSIONS

The crystallization kinetics of poly(*p*-phenylene sulphide) were studied as a function of molecular weight. The linear crystal growth rate and the overall rate of bulk crystallization were analysed. The overall rate of bulk crystallization was described by a single Avrami equation with exponent ~3. In the range of molecular weights studied, both crystal growth rates and overall rates of bulk crystallization decreased by a factor of 4 as the molecular weight increased, at a supercooling of 70°C. Values of linear crystal growth rates and overall rates of crystallization were combined to calculate the nucleation density as a function of crystallization temperature. The results showed a 32-fold lower nucleation density in the case of low molecular weight PPS24.

The crystal growth rate data were analysed as a function of the molecular weight. These data seemed to represent another example that follows a logarithmic function of the number average molecular weight proposed by Cheng and Wunderlich[28].

ACKNOWLEDGEMENTS

The authors are grateful to Dr C. J. Stacy for sharing the well characterized samples utilized in this study, to Dr

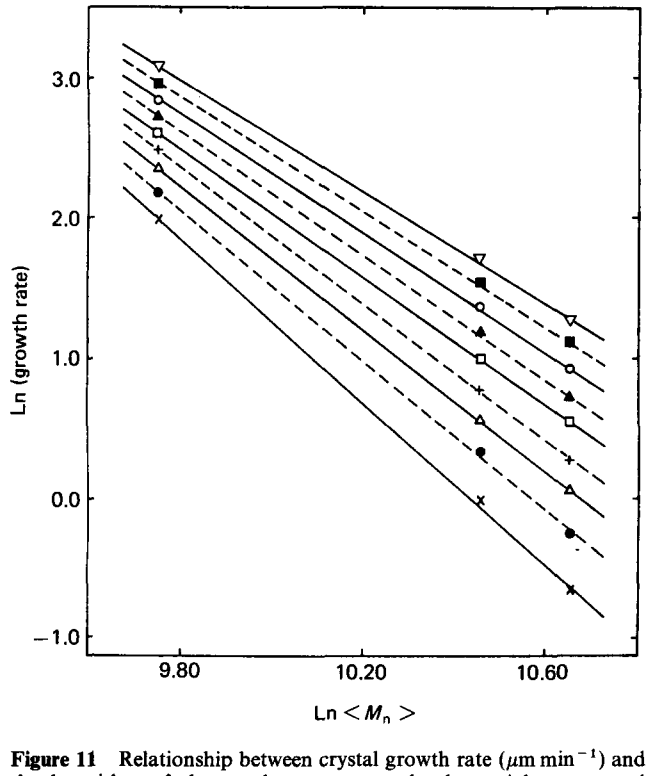

Figure 11 Relationship between crystal growth rate (μm min^{-1}) and the logarithm of the number-average molecular weight at several supercoolings (following equation (11)). ΔT (°C): ×, 60.0; ●, 62.5; △, 65.0; +, 67.5; □, 70.0; ▲, 72.5; ○, 75.0; ■, 77.5; ▽, 80.0

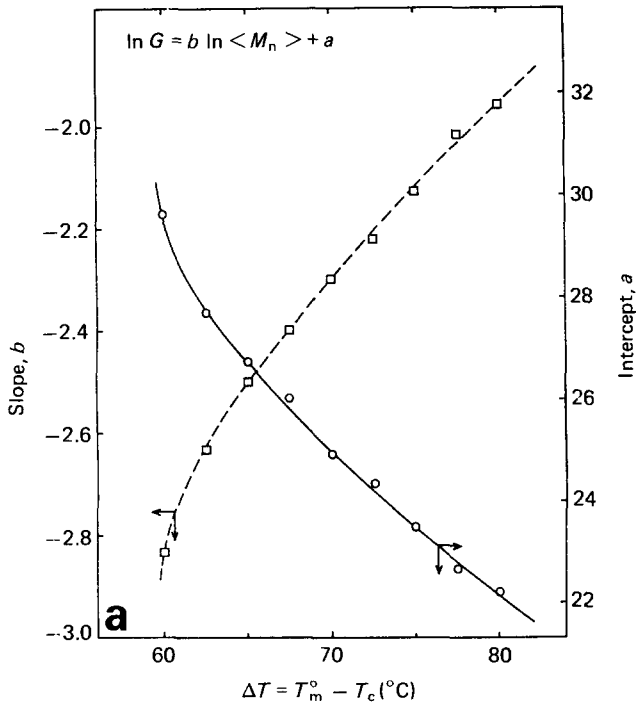

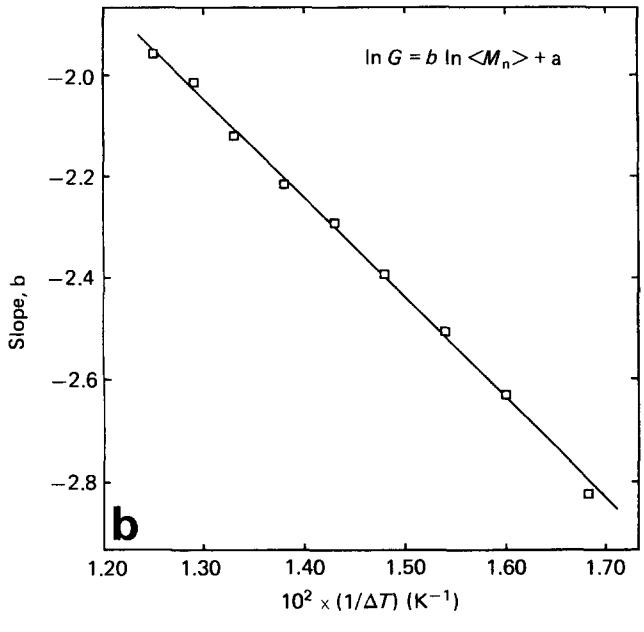

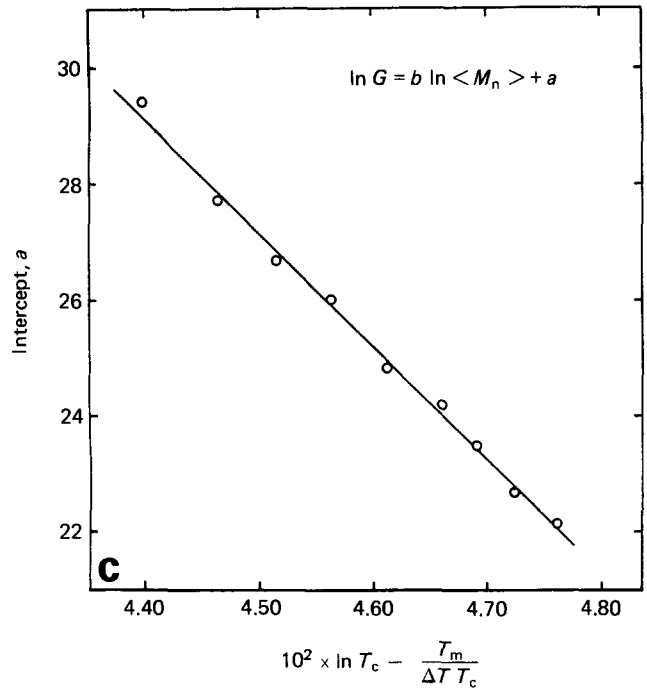

Figure 12 Slopes and intercepts of the linear relationship between logarithm of crystal growth rate and logarithm of the number-average molecular weight extracted from *Figure 11*. (a) Slope and intercept vs. supercooling, ΔT; (b) slope vs. $1/\Delta T$; (c) intercept vs. $\ln T_c - (T_m^0/\Delta T T_c)$

J. F. Geibel for interesting discussions and to the Phillips Petroleum Company for their financial support.

REFERENCES

1 Hill Jr, H. W. and Brady, D. G. *Polym. Eng. Sci.* 1976, **16**, 832
2 Short, J. N. and Hill Jr, H. W. *Chem. Technol.* 1972, **2**, 481
3 Brady, D. G. *J. Appl. Polym. Sci., Appl. Polym. Symp.* 1981, **36**, 231
4 Shue, R. S. *Dev. Plast. Technol.* 1985, **2**, 259
5 Clarke, T. C., Kanazawa, K. K., Lee, V. Y., Rabolt, J. F., Reynolds, J. R. and Street, G. B. *J. Polym. Sci., Polym. Phys. Edn.* 1982, **20**, 117
6 Frommer, J. E., Elsenbaumer, R. L., Eckhardt, H. and Chance, R. R. *J. Polym. Sci., Polym. Lett. Edn.* 1983, **21**, 39
7 Schoch Jr, K. F., Chance, J. F. and Pfeiffer, K. E. *Macromolecules* 1985, **18**, 2389
8 Jog, J. P. and Nadkarni, V. M. *J. Appl. Polym. Sci.* 1985, **30**, 997
9 Lovinger, A. J., Davis, D. D. and Padden Jr, F. J. *Polymer* 1985, **26**, 1595
10 Zeng, H. and Ho, G. *Angew. Makromol. Chem.* 1984, **127**, 103
11 Brady, D. G. *J. Appl. Polym. Sci.* 1976, **20**, 2541
12 Waddon, A. J., Hill, M. J., Keller, A. and Blundell, D. J. *J. Mater. Sci.* in press
13 López, L. C. and Wilkes, G. L. *J. Polym. Sci., Polym. Lett. Edn.* 1986, **24**, 573
14 Hawkins, R. T. *Macromolecules* 1976, **9**, 189
15 Hoffman, J. D., Davis, G. T. and Lauritzen Jr, J. I. in 'Treatise on Solid State Chemistry' (Ed. N. B. Hannay), Plenum Press, New York, 1976, Vol. 3, Ch. 7
16 Lauritzen Jr, J. I. and Hoffman, J. D. *J. Appl. Phys.* 1973, **44**, 4340
17 Hoffman, J. D. *Polymer* 1983, **24**, 3
18 Avrami, M. *J. Chem. Phys.* 1939, **7**, 1103; *J. Chem. Phys.* 1940, **8**, 212; *J. Chem. Phys.* 1941, **9**, 177
19 Wunderlich, B. 'Macromolecular Physics, Crystal Nucleation, Growth, Annealing', Vol. 2, Academic Press, New York, 1976
20 Price, F. P. *J. Polym. Sci.* (A) 1965, **3**, 3079
21 Van Antwerpen, F. and van Krevelen, D. W. *J. Polym. Sci., Polym. Phys. Edn.* 1972, **10**, 2423
22 Lauritzen Jr, J. I. and Hoffman, J. D. *J. Res. Natl. Bur. Stand.* (*A*) 1960, **64**, 73
23 Devoy, C. and Mandelkern, L. *J. Polym. Sci.* (*A-2*) 1969, **7**, 1883
24 Lovering, E. G. *J. Polym. Sci.* (*C*) 1970, **30**, 329
25 Hoffman, J. D. and Weeks, J. J. *J. Chem. Phys.* 1962, **37**, 1723
26 Hoffman, J. D. *Polymer* 1982, **23**, 656
27 Magill, J. H. and Li, H. M. *Polymer* 1978, **19**, 416
28 Cheng, S. Z. D. and Wunderlich, B. *J. Polym. Sci., Polym. Phys. Edn.* 1986, **24**, 595
29 Hoffman, J. D. and Weeks, J. J. *J. Res. Natl. Bur. Stand* (*A*) 1962, **66**, 13
30 Stacy, C. J. *J. Appl. Polym. Sci.* 1986, **32**, 3959